SCIENTIFIC PAPERS
OF THE UNIVERSITY OF PARDUBICE
Series A
Faculty of Chemical Technology
18 (2012)

DECONVOLUTION OF COMPLEX CRYSTALLIZATION PROCESSES: AMORPHOUS SELENIUM

Roman SVOBODA[1] and Jiří MÁLEK
Department of Physical Chemistry,
The University of Pardubice, CZ–532 10 Pardubice

Received September 6, 2012

Crystallization behavior of the selenium glass was studied by means of the differential scanning calorimetry under non-isothermal conditions. Two new approaches to the evaluation of crystallization kinetics — advanced interpretation of characteristic kinetic functions and modified Fraser–Suzuki deconvolution — were applied. The determination of kinetic parameters in the dependence on particle size can provide an extensive amount of information about the nature of the involved surface and bulk crystallization mechanisms. Based on these information, the deconvolution in terms of the Johnson–Mehl–Avrami process was performed, separating the two mechanisms. The results not only both, qualitatively and quantitatively, describe the crystallization process in glassy selenium but also explain various data from literature on this topic. Introduced deconvolution may represent a new approach to gaining information about complex crystallization processes for numerous material science applications.

[1] To whom correspondence should be addressed.

Introduction

Crystallization processes belong among the most important phenomena, both studied and utilized within the field of material sciences. From this point of view it is obvious that the studies of crystallization kinetics are of significant importance. Nowadays, the most common tool for this task is a differential scanning calorimeter (DSC). For the case of a single-process peak, the kinetic equation of DSC curve can be described [1] as follows

$$\Phi = \Delta H A e^{-E/RT} f(\alpha) \tag{1}$$

where Φ is the measured heat flow, ΔH is the crystallization enthalpy, A is the pre-exponential factor, E is the apparent activation energy of the process, R is the universal gas constant, T is temperature and $f(\alpha)$ stands for an expression of a kinetic model with α being conversion.

In the first step of kinetic analysis, the apparent activation energy E is usually calculated. In our work, the original Kissinger method and isoconversional Friedman method are applied. The Kissinger equation [2] is based on an assumption that the conversion degree, α, corresponding to the maximum crystallization rate is a constant and does not depend on experimental conditions. The apparent activation energy of the crystallization process in this case can be determined only for non-isothermal measurements and is proportional to the slope of the dependence of the temperature corresponding to the maximum of the crystallization peak T_p (i.e., point of the maximum conversion rate) on the applied heating rate q^+. This dependence can be described according to Kissinger by Eq. (2)

$$\ln \frac{T_p^2}{q^+} = -\frac{E}{R T_p} + \text{const.} \tag{2}$$

The second used evaluation method is that developed by Friedman [3]. This is, contrary to the Kissinger equation, an isoconversional method, where the assumption of the conversion rate, α, being constant at the crystallization peak maximum for all heating rates is taken and the Friedman method is based directly on the premise to this assumption. In other words, the activation energy is calculated for various chosen degrees of conversion and then averaged (usually for the interval of α = 0.3-0.7, where the influence of experimental conditions is minimized — in contrast to the peak tails). The Friedman equation may be expressed as

$$\ln \Phi_\alpha = -\frac{E}{R T_\alpha} + \text{const.} \tag{3}$$

where Φ_α and T_α are the values of the heat flow and temperature, respectively, for chosen degree of conversion, α, and a given heating rate.

In the second step of kinetic analysis, an appropriate kinetic model needs to be determined. Málek [4,5] introduced a method to test applicability of various kinetic models to experimental data. The kinetic file data (T-Φ-α) for non-isothermal conditions are transformed according to Eqs (4) and (5) and displayed as the $z(\alpha)$ or $y(\alpha)$ functions versus α

$$y(\alpha) = \Phi e^{E/RT} \tag{4}$$

$$z(\alpha) = \Phi T^2 \tag{5}$$

The data are usually normalized on both axes for a better clarity when comparing a whole set of curves measured at different heating rates. In order to determine an appropriate kinetic model from the $y(\alpha)$ and $z(\alpha)$ functions, the conversion rates corresponding to their maxima, $\alpha_{max,y}$ and $\alpha_{max,z}$, have to be found. These values are characteristic for each kinetic model; the algorithm mentioned in, e.g., Ref. [5] summarizes the characteristic maxima for several most typical kinetic models.

In this regard, one of the most widely used kinetic models for description of the crystallization processes in glasses is the nucleation-growth Johnson–Mehl–Avrami model, JMA(m) [6-9]

$$f(\alpha) = m(1 - \alpha)[-\ln(1 - \alpha)]^{1-(1/m)} \tag{6}$$

where m is the parameter reflecting nucleation and crystal growth mechanisms as well as the crystal morphology. The main advantage of this model is the parameter m having physical meaning.

The JMA kinetic parameter m can be determined according to the following two equations. In the first method, the JMA parameter is calculated from the conversion corresponding to the maximum of the $y(\alpha)$ function $\alpha_{max,y}$ according to [10]

$$m = \frac{1}{1 + \ln(1 - \alpha_{max,y})} \tag{7}$$

An alternative way of determination of parameter m is using a double logarithm function [11]

$$\frac{d\ln[-\ln(1 - \alpha)]}{d(1/T)} = \frac{mE}{R} \tag{8}$$

In addition, linear dependence of this equation is also often considered a satisfactory condition for the applicability of the JMA model. Advantages and disadvantages of both mentioned methods were discussed in detail in Ref. [12].

In the last step of enumerating the quantities in Eq. (1), the pre-exponential factor A is determined. In our work, this was done by means of the curve-fitting of the experimental data — Equation 1 with the value of A being the only variable was employed in this task. The minimum of the residual sum of squares was sought to obtain the best fit.

The above mentioned procedure is, of course, just one of possible solutions. The modern kinetic analysis disposes of numerous tools for an evaluation of the kinetic parameters; among the probably most famous evaluation methods belong: master plots [4,5,13], non-parametric analysis [14,15], combined kinetic analysis [16,17] or invariant kinetic parametrization [18,19]. All these methods are very well developed and provide reliable and accurate results for any type of the kinetic process. However, all these methods were, obviously, derived for a solitary process and usually fail when applied in a situation with complex or multiple overlapping processes. In the case of such complex processes, usually a nonlinear re-gression is applied in order to determine kinetic parameters of the involved processes from an overall response by gradual optimization. Nevertheless, such approach may increasingly suffer from influences of thermal gradients and data acquisition imperfections. Second way how to treat the data corresponding to overlapping processes is represented by a separation of the individual processes in a peak-deconvolution procedure and consequent application of kinetic analysis methods to the separated peaks. The latter approach was recently significantly improved by Perejón *et al*. [20], who suggested the application of the Fraser–Suzuki function [21,22] in the deconvolution procedure. In their paper, Perejón *et al*. performed extensive comparative testing of various conventional mathematical functions in order to determine a suitable equation capable of accu-rate and independent fit of data generated on the basis of all common kinetic models. The deconvolution procedure using Fraser–Suzuki function together with the subsequent application of combined analysis were successfully tested on both simulated and experimental data corresponding to overlapping processes, where in all the cases a correct kinetic model and values of kinetic parameters were determined.

In our work, we would like to further improve the application of the method suggested by Perejón *et al*. [20] for the case of crystallization kinetics by considering the specificities of the crystallization processes in glasses and implementing several constraining conditions. The new introduced method will be tested on the data corresponding to crystallization of amorphous selenium. This material was chosen among other also for the fact that even though it is a fundamental and often also considered "model" material, the published literature dealing with crystallization of a-Se still contains questions and discrepancies and no general consensus regarding the values of kinetic parameters has been reached [23-28].

Experimental

The amorphous selenium was prepared by a melt-quenching technique from the pure element. Approximately 10 g selenium pellets (5N, Sigma Aldrich) were inserted into a fused silica ampoule; the ampoule was degassed and sealed afterwards. The batched ampoule was annealed in rocking furnace at 650 °C for 24 h and then quenched in water. Amorphous nature of the glass was checked by X-ray diffraction. The prepared glass was ground and the obtained powder was sieved and distributed according to particle size into the following fractions: 0-20, 20-50, 50-125, 125-180, 180-250, 250-300 and 300-500 μm. In addition, also bulk samples were prepared by cracking a layer of as-prepared bulk glass right after its removing from the ampoule. Bulk samples were assigned the average particle size d_{aver} = 1 mm for comparison reasons. Each fraction was studied separately, and its kinetic analysis was performed independently.

The crystallization processes in the prepared powder fractions were studied by a conventional differential scanning calorimeter DSC 822^e (Mettler, Toledo) equipped with a cooling accessory. Dry nitrogen was used as the purge gas at the rate of 20 cm^3 min^{-1}. Temperature, the heat flow and τ-lag calibrations of the calorimeter were performed on the basis of the melting of In, Zn and Ga. A baseline was checked daily. A thin layer of the powder was always spread on the bottom of aluminum pans to improve thermal contact, and at the same time, to minimize the variety of the heat transfer processes. Masses of the powder samples varied in-between 8-10 mg; in the case of bulk samples, the masses were approximately 20 mg.

Regarding the applied temperature program, in the case of selenium glass the crystallization process is jeopardized from both sides. At a low temperature side the glass transition tends to intervene with the crystallization; at the high temperature side it is the melting of the crystalline phase that may overlap with the end of the crystallization peak. The influence of the glass transition was eliminated in our work by suppression of the relaxation effects — the sample was first subjected to a 5 min isotherm at 50 °C, where the material reached thermally and structurally the equilibrium state of undercooled liquid (thus whole previous thermal history was erased and corresponding relaxation effects eliminated); this short period of time also served as a pre-nucleation step. In the second step, the sample was cooled to 10 °C at the rate of 10 °C min^{-1}; and finally a heating step to 250 °C was applied. The cooling step was inserted in order for the linear heating rate to be established before reaching the temperatures critical for nucleation and crystal growth even for the highest heating rates. Concerning the intervention of the melting process, in the case of the highest heating rates and the coarsest powder fractions, the crystallization peak end-tail started to turn directly into the melting, which may slightly affect the ΔH_{cry} value for these samples (the kinetics follows the trend given by lower heating rates and, therefore, does not seem to be

influenced at all). The applied heating rates were: 1, 2, 3, 5, 7, 10, 15, 20 and 30 °C min^{-1}.

Prior to the evaluation of kinetic analysis, the data corresponding directly to the heat evolved during the crystallization needed to be acquired. As the difference between the undercooled liquid and crystal heat capacities is not negligible, the simple linear baseline approximation could not be used. In our recent work [12,29,30], where more detailed discussions on this topic are presented, it was found that spline-type baselines imitate very well various thermodynamic backgrounds. This was confirmed also for the glass studied within the framework of this article.

Results and Discussion

This section is going to be divided into three parts. In the first part the modified Fraser–Suzuki deconvolution will be reviewed and particular modifications associated with the current study on amorphous selenium will be introduced. In the second part, the actual kinetic results for a-Se will be shown — first the interpretation of characteristic kinetic functions will be applied and then the actual FS deconvolution (based on the information from the latter) will be performed. In the last part, the obtained results and achieved conclusions will be compared with literature data.

Modified Fraser–Suzuki Deconvolution

The treatment of complex crystallization processes, where overlapping of signals corresponding to multiple processes/mechanisms occurs, is of very high interest for the scientific field of thermal analysis. Recently, a Fraser-Suzuki function was tested as a suitable deconvolution function for complex kinetic processes measured by DSC, DTA or DTG [20]. It is well known that in practice it is mostly only the Johnson–Mehl–Avrami and Šesták–Berggren models that apply to the description of crystallizations in glasses. However, the peak-fitting procedure representing the initial step of kinetic analysis approach introduced by Perejón *et al*. [20] is very sensitive to inaccuracies and systematic errors in the experimental data, which may (though slightly) distort the true crystallization process response. Nevertheless, even a slight distortion of the fitted curve may eventually lead to the determination of incorrect kinetic parameters or even to suggestion of a wrong kinetic model (due to an incorrect deconvolution), if the highest correlation coefficient is the only criterion of the best fit. In this regard, it may be advantageous to introduce certain restricting conditions into the deconvolution procedure in order to reduce the number of outcomes only to those “physically meaningful”, even though the

correlation coefficient of such fit will not be the highest possible. In particular, we have introduced [31] a method of conversion of the general Fraser–Suzuki function suggested in [10] into the direct fit by the JMA model.

It was shown by Perejón *et al*. [10] that the Fraser–Suzuki function is suitable for the deconvolution procedure of complex and overlapping processes as this function can very well describe (fit) data corresponding to all commonly used kinetic models. The Fraser–Suzuki function can be expressed as

$$y = a_0 \exp\left[-\ln 2\left[\frac{\ln\left(1 + 2a_3\dfrac{x - a_1}{a_2}\right)}{a_3}\right]^2\right] \tag{9}$$

where a_0, a_1, a_2 and a_3 are the parameters corresponding to the amplitude, position, half-width and asymmetry of the curve, respectively. In practice (as the Fraser–Suzuki expression is a peak-fitting function), the input data for the deconvolution procedure need to be expressed in the form of the temperature dependence of a property proportional to the conversion rate, $\mathrm{d}\alpha/\mathrm{d}t$, (heat flow from DSC, mass loss from DTG, *etc*.). In addition, to the present authors' knowledge the function was so far tested only for non-isothermal conditions — in the case of isothermal data the peak shape is considerably different. For this reason, our study is limited to the non-isothermal data too.

In order to find a correlation between the JMA model and Fraser–Suzuki function, first a number of theoretical curves were simulated using the general expression for conversion rate of a kinetic process

$$\frac{\mathrm{d}\alpha}{\mathrm{d}t} = A e^{-E/RT} f(\alpha) \tag{10}$$

where A is a pre-exponential factor, E is the apparent activation energy, R is the universal gas constant, T is temperature and $f(\alpha)$ stands for a kinetic model function. Instead of the kinetic model function, the expression for the JMA model (Eq. (6)) was used with the following values of the kinetic parameter m: 1, 1.5, 2, 2.5 and 3. For each value of parameter m, a matrix/set of theoretical curves was simulated using combinations of the following values of $\ln A$ and E: the logarithm of the pre-exponential factor varied in the range from 15 to 40 (with a graduation step of 5 units), apparent activation energy varied in the range from 60 to 260 kJ mol^{-1} (with a graduation step of 20 kJ mol^{-1}). As already above mentioned, the curves were simulated in non-isothermal regime — for each combination of parameters two heating rates (3 °C min^{-1} and 10 °C min^{-1}) were applied. Altogether

660 different curves based on the JMA model were prepared.

In the second step, all the simulated JMA curves were fitted by the Fraser–Suzuki function. For this reason, a computer program Peakfit (Systat Software Inc.) was used. The parameters of the FS function were obtained through a non-linear optimization method by using the Levenberg–Marquardt algorithm. The minimum of the residual sum of squares *RSS* was sought in order to obtain the best fit. All the correlation coefficients were higher than 0.9999. For each fit, apart from the values of FS parameters, also certain peak characteristics were obtained — namely the peak amplitude (equal to parameter a_0), peak center (equal to parameter a_1), full width at half-maxima (value very close to parameter a_2), full width at peak base, asymmetry at half-maxima and asymmetry at 10 % of peak maxima.

In the third, last and the most important step, a suitable peak characteristic was chosen in order to correlate the results obtained from the fitting procedure by using the Fraser–Suzuki function with actual physical response corresponding to the Johnson–Mehl–Avrami model. It is obvious that the peak amplitude, position or width at half-maxima (and, as a consequence, also parameters a_0, a_1 and a_2) depend also on the values of activation energy and pre-exponential factor and, therefore, cannot be used as a simple even though fast characterization of the JMA process. In this regard, it should be mentioned that the product of parameters a_0 and a_2 (peak amplitude and approximate width at half-height) in the case of the JMA model gives a constant value 0.894 ± 0.005 (calculated for all 660 simulated JMA curves), thus effectively reducing the number of parameters in the Fraser–Suzuki function by one. However, in order for the parameters to give this value, the data need to be in the reduced form of the pure conversion rate, $d\alpha/dt$ — i.e., in the case of, e.g., a DSC signal obtained in W g^{-1} the data would have to be first divided by the enthalpy corresponding to the studied process (in J g^{-1}). In addition, most importantly, the above mentioned product is not unique with respect to the applied kinetic model: a similar value may also be obtained in the case of certain other models — from this point of view, it can be concluded that the ($a_0 \times a_2$) product is not a suitable characteristic for the JMA model.

On the other hand, on the basis of the curve-fitting of the theoretical JMA curves, we found that all these peaks have characteristic asymmetry mean value of parameter a_3 calculated from all the 660 JMA curves was –0.357 ± 0.021. The advantage of this parameter is also in the fact that the asymmetry of the peak does not depend on the measured property as long as the studied process follows the JMA kinetics. In other words, this characteristic of the JMA process using the Fraser–Suzuki fit is generally applicable to all TA techniques (DSC, DTG, differentiated TMA signal, *etc*.). In a crucial reverse simulation study, we also confirmed that every Fraser–Suzuki function with fixed parameter a_3 = 0.357 corresponds to the JMA kinetics, regardless of the values of the other three parameters (a_0, a_1 and a_2). The JMA kinetics was confirmed using the characteristic kinetic function $z(\alpha)$ [4,5] for all reasonable combinations of FS parameters. In all

the cases, the maximum of the $z(\alpha)$ function corresponded to the value characteristic for the JMA model (theoretical JMA "fingerprint" value is $\alpha_{max,z} = 0.632$). This means that this characteristic is truly universal, and the asymmetry of the JMA model (and in consequence, the value of FS parameter a_3) can be used to quickly test the JMA model applicability. In accordance with our study, this also means that in the case of complex overlapping crystallization processes the deconvolution procedure using the Fraser–Suzuki function with restricted parameter a_3 can effectively turn into a fit by using the JMA model even though no other kinetic parameters (E, A or m) are known. In addition, this also to a certain extent solves the question of undesirable thermal gradients occurring during measurements or improper data acquisition prior to the deconvolution procedure.

Application to a-Se Crystallization Data

It was shown in our earlier work that the so-called "advanced interpretation of characteristic kinetic functions $z(\alpha)$ and $y(\alpha)$" may provide extensive amount of extra information about the crystallization mechanism (in addition to the basic set of kinetic parameters obtained by the conventional kinetic analysis). In fact, according to our findings, this additional information seems to be extremely helpful for successful and reliable deconvolution in the case of fully overlapping processes.

In this regard, first the activation energy was investigated by means of the so called Kissinger plots. The evaluation according to Kissinger equation (Eq. (2)) for all the studied particle size fractions is displayed in Fig. 1. It can be very clearly seen that for the increasing particle size the dependencies gain convex curvature, i.e., the peak maxima for the high heating rates are shifted to temperatures higher than those corresponding to the linearity observed for fine powders. This phenomenon usually corresponds to either a change in the crystallization mechanism or a shift resulting from thermal gradients in the sample or DSC cell. As the DSC instrument time constant was properly calibrated, the thermal contacts were maximized (see Experimental part), and similar materials (alike chemical structure and thermal properties including thermal conductivity and heat capacity) measured under similar conditions (the same heating rates, similar sample masses) in our earlier work (see, e.g., Ref. [12]) did not show this curvature, it can be safely assumed that the thermal gradients were eliminated and the dependence curvatures are a true response of the measured material. However, in such case a problem arises for the following kinetic analysis, where ideally a uniform value of activation energy is needed to be assigned to the studied process. Bearing in mind that an *apparent* activation energy is being evaluated, a possible solution might be to determine E for each heating rate separately from the slope of the corresponding

tangent line. On the other hand, such solution would not correctly represent the fact that the temperature corresponding to the maximum of the crystallization peak is very robust value invariable to most experimental conditions (thus reflecting the true response of the material), which, however, in most cases corresponds to the dominant crystallization mechanism. Therefore, without deeper knowledge of the relationship between the involved mechanisms, it is better to consider, in the first approximation, a uniform value of E corresponding to the leading process (in this case that manifesting at low heating rates), than to introduce an additional parameter of varying activation energy in the subsequent interpretation of characteristic kinetic functions.

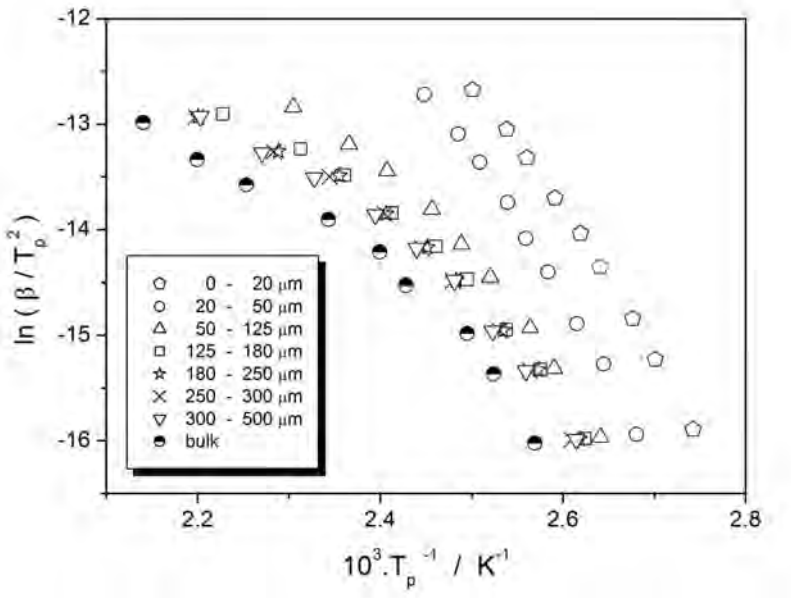

Fig. 1 Determination of apparent activation energy of crystallization process according to Kissinger method for all studied selenium particle size fractions. Overall crystallization response is evaluated

The Kissinger plots depicted in Fig. 1 were used to determine the apparent activation energy, E, according to Eq. 2. The data corresponding to low heating rates were taken for the reasons explained in the previous paragraph. The resulting values of E are depicted in Fig. 2 (circles) as a function of the average particle size. Nevertheless, for the further comparison also the activation energies corresponding to the high heating rates data were evaluated — squares in Fig. 2. It can be seen that the difference is significant; this will be commented later. For the reasons of the advanced interpretations described in this subsection, the activation energies determined from low q^+ data were used. On a related topic, the present authors would like to remark that in case of unknown thermal properties of a material or DSC cell the low heating rates should always be used to evaluate the activation energy, E, due to the unknown possible influence of thermal gradients present at higher heating rates (which was, however, not the case of our data).

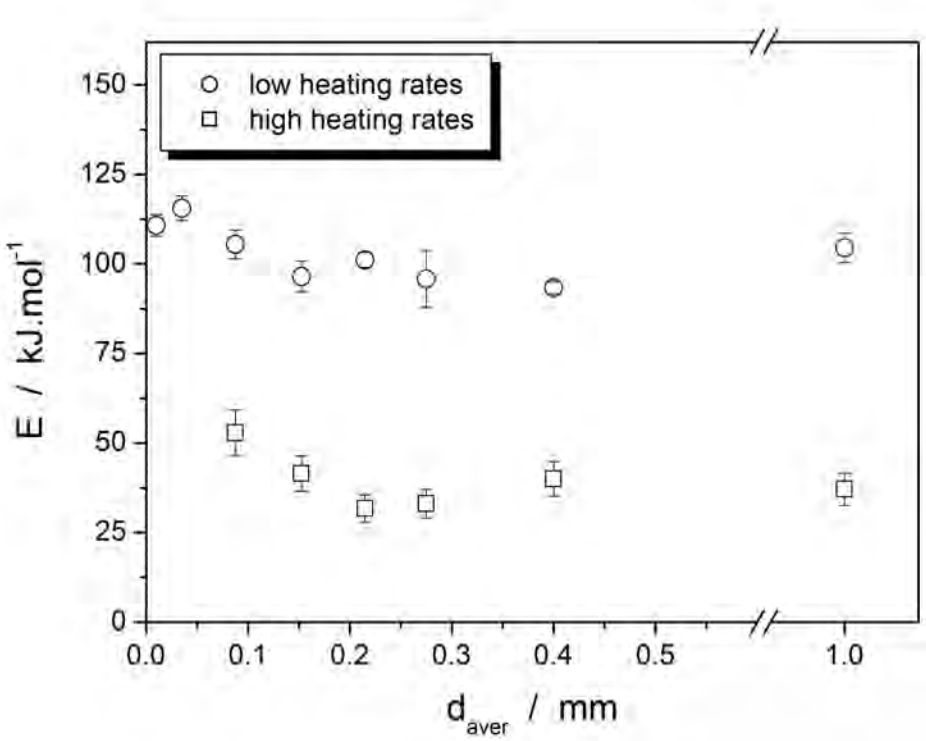

Fig. 2 Comparison of apparent activation energies determined for glassy selenium according to Kissinger equation in dependence on average particle size in particular fractions. Bulk samples were assigned d_{aver} = 1 mm. Evaluations based on data corresponding to low/high heating rates are shown as two respective separate dependences

In a continuation of the crystallization kinetics evaluation, the proper reaction model needs to be determined. In Fig. 3, an example of the normalized characteristic kinetic functions $z(\alpha)$ and $y(\alpha)$ is depicted for several chosen particle size fractions — curves corresponding to all the applied heating rates are always shown. For the kinetic model to be determined, the value of the degree of conversion corresponding to the maximum of $z(\alpha)$ function is critical. The values of $\alpha_{max,z}$ characteristic for the most typical kinetic models can be found, e.g., in Ref. [5]. Málek showed that for the most common kinetic model — Johnson–Mehl–Avrami (JMA) — to be applicable, the $\alpha_{max,z}$ has to be equal to 0.632, which is a characteristic "fingerprint" of the JMA model. Nonetheless, it was shown [12,29] that in certain cases the JMA model can provide a very good description of experimental data even when $\alpha_{max,z}$ value is outside the limits of (0.62-0.64) originally suggested by Málek. In the case of all the studied particle size fractions, it was apparent that the maxima of all $z(\alpha)$ functions were very close to the value $\alpha_{max,z}$ = 0.632, suggesting applicability of the JMA model.

The first aspect to consider within the advanced interpretation approach is the reproducibility of characteristic kinetic functions for each particle size fraction with respect to the changing heating rate. The changing shape of $z(\alpha)$ function or position of the $\alpha_{max,z}$ is generally undesirable and may be associated with either a change in the kinetic model or with a pronounced influence of thermal gradients

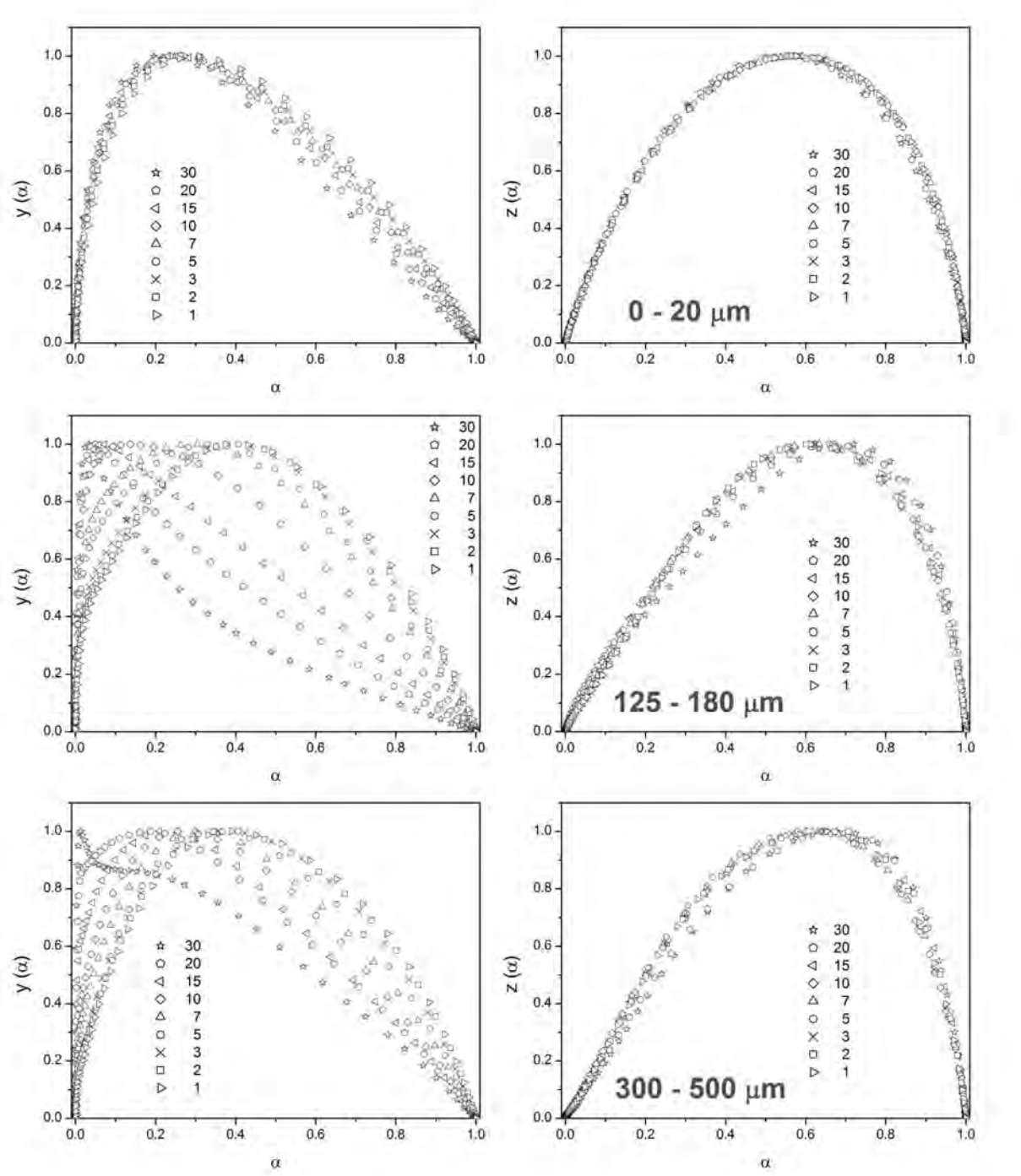

Fig. 3 Normalized $y(\alpha)$ and $z(\alpha)$ functions corresponding to non-isothermal measurements of chosen particle size fractions of the selenium glass. Particular rows match the individual studied fractions. The overall crystallization response is evaluated

and lagging. In the case of a significant change in the kinetic model with the heating rate, an overlapping of two mutually interacting unrelated processes is possibly the most probable option — nevertheless this interaction will also manifest itself in the change of $y(\alpha)$ function shape, which can make the following conclusions regarding the change in the process mechanism unreliable. Similarly, the influence of thermal gradients may distort the crystallization peaks and make

the kinetic analysis provide wrong and biased results. In the case of significant thermal gradients being present, the identification of their origin is crucial for both, their elimination or accounting for them in at least qualitative kinetics interpretation. Anyhow, both above mentioned situations should be recognized and carefully accounted for in consequent interpretations or process separations. In the case of the data obtained for a-Se studied in our work, it can be seen that all the $z(\alpha)$ functions are perfectly consistent for each particle size fraction, with the only exception being occasional slight shift of the curve corresponding to the highest heating rates, where some small distortions due to insufficient thermal contact or transport would already be acceptable.

On the other hand, inconsistency of the shape of $y(\alpha)$ function with heating rate for a single studied fraction is not unusual and provides information about the overall crystallization mechanism changing due to differing representation intensity of overlapping crystallization processes/mechanisms as a consequence of different values of their apparent activation energy, E, and the pre-exponential factor, A. With regard to the data shown in present article, it can be seen that for the 0-20 μm and bulk fractions the shape of $y(\alpha)$ function is relatively consistent, which implies a strong domination of a single crystallization mechanism (surface crystallization in the case of the 0-20 μm fraction, volume crystallization in the case of bulk sample). On the other hand, in the case of all other studied fractions, the curves are systematically changing with the heating rate, meaning a significant representation of both discussed mechanisms.

In the second considered aspect of advanced interpretations of characteristic kinetic functions, the variability of the $y(\alpha)$ function with the particle size is explored. For this reason, the values of $\alpha_{max,y}$ and $\alpha_{max,z}$ can be either plotted in the dependence on the average particle size or a combined kinetic plot as that shown in Fig. 4 can be created. In Fig. 4 it can clearly be seen that the "averaged" overall mechanism shifts with the particle size towards higher values of $\alpha_{max,y}$, i.e., the crystallization dimensionality increases. This again corresponds to the concept of the surface crystallization being dominant for fine powders (large portion of material includes surface defects and crystallization centers typical for surface crystallization) and volume crystallization manifesting dominantly in the case of coarse powders, where the major part of the glass grain is in the bulk form with minimum mechanical defects or stresses being present. An exception, from this generally assumed concept, is the data for the finest particle size fraction 0-20 μm that shows slightly higher dimensionality than corresponds to the other fine powders. Similar observation was, however, made in our earlier work for the $Se_{70}Te_{30}$ glass, where this phenomenon was explained on the basis of steric restrictions forcing the individual crystallites to grow throughout the whole grain, hence showing virtually higher dimensionality [29]. In addition, it is further apparent from the figure that all the data including their error bars lie in a close vicinity of the original narrow JMA model applicability interval suggested by Má-

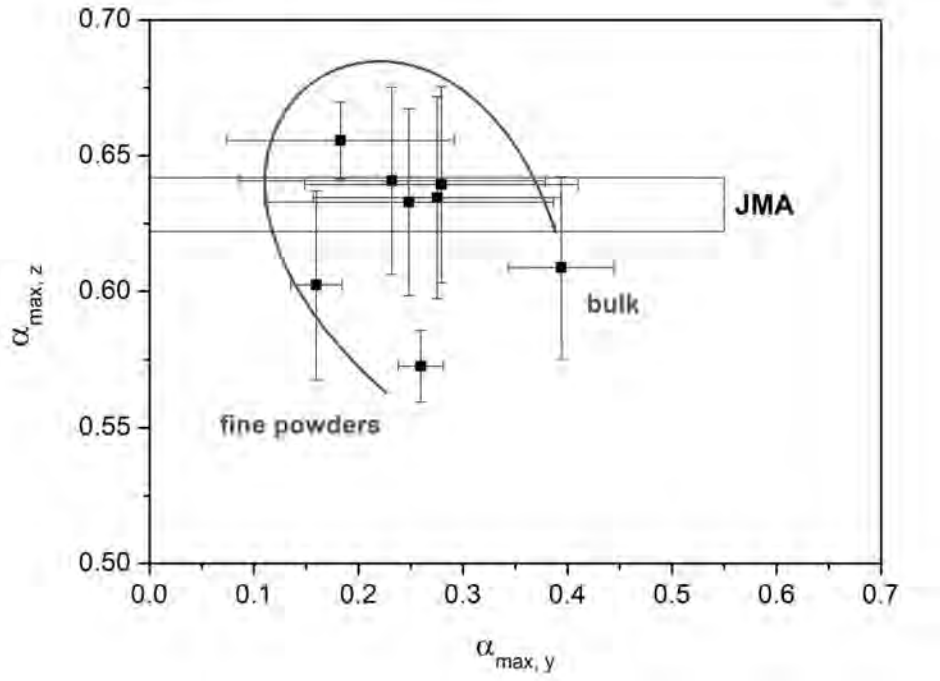

Fig. 4 So called "kinetic plot" evaluated for selenium glass. Theoretical applicability of JMA model as suggested by Málek [4] is displayed. Solid curve guides eyes in direction of increasing particle sizes in particular fractions

lek, i.e., the Johnson–Mehl–Avrami model should provide reasonable description of the crystallization data.

Within the framework of the third, the most important considered aspect, the overall trends in the crystallization responses are identified and the involved mechanisms are qualitatively described for the complex crystallization process. Based on the $y(\alpha)$ and $z(\alpha)$ functions, the following interpretations can be made. In the case of amorphous selenium, both basic crystallization mechanisms — surface and bulk — are significantly represented in the overall devitrification transformation. Their proportion is driven by the initial ratio between the numbers of crystallization centres corresponding to the particular mechanisms. In the case of the finest fraction 0-20 μm, there are no signs of the bulk crystallization mechanism being present, the glass grains are so small that the entire particle is composed of the material containing a high number of mechanical defects, which in addition are subjected to large amounts of strain and stress. In addition, this type of mixed "surface" crystallization behavior seems to lead to the typical rounded shape of the $z(\alpha)$ function (similar behavior was observed for $Ge_2Sb_2Se_5$ glass [30]). For all the other particle size fractions, there is an apparent simultaneous presence of the bulk crystallization process, the manifestation of which increases with an increasing particle size (higher amounts of true "bulk" material containing nuclei). It is further apparent that the heating rate plays a crucial role in the relative representation of the two proceeding types of crystallization — for low heating rates the bulk crystallization mechanism is more pronounced and *vice versa*. In

order to explain this phenomenon, the difference in the activation energies of the two involved processes will be employed.

It is apparent from Fig. 1 that the surface crystallization appears to have slightly but still significantly higher activation energy than the bulk process. In addition, the three-dimensional kinetics is axiomatically slower and can be further decelerated by, e.g., steric reasons. As it can already be seen from Fig. 3 (and as will be proven later), the first process that corresponds to the earliest heat evolution is always the surface crystallization. Therefore, during the fast heating, the starting primary surface crystallization mechanism takes control over the larger partition of the complex crystallization process (with more than enough energy being provided by the faster heating and thermal gradients causing the whole process to be allocated to higher temperatures), while the slower bulk mechanism does not have enough time to fully develop (in accordance with the concept of competing processes). Correspondingly, at low heating rates, it is the difference in the activation energies that determines the outcome. Although it is still the surface crystallization that starts the complex crystallization, the energy input (caused by the factual temperature increase plus the heat evolved during the crystallization) is relatively low and an actual competition based on the difference between energy barriers (represented by the apparent activation energy E_A) takes place, causing the bulk process to be more pronounced while "consuming" a larger part of the provided energy.

Furthermore, a piece of information about the relative position of the peaks representing the respective involved processes can be extracted from the shape of $y(\alpha)$ function. In particular, it is the dominant crystallization mechanism with respect to the degree of conversion α, which is identified. This effect is the most apparent for the 30 °C min^{-1} heating rate and coarse powders, where the independence of the surface and bulk crystallization processes can be assumed. In such case, even partial separation of the two processes (with respect to their mutual position on temperature axis) results in a characteristic shape of the $y(\alpha)$ function. This characteristic shape, as will be proved later, is caused by, and corresponds to, the extent of separation rather than the ratio between actual intensities of processes. Nonetheless, it has to be borne in mind that this characteristic shape corresponding to the partially separated/shifted processes appears only if the mechanisms differ in their kinetics significantly. The opposite situation (only partially overlapping peaks of comparable areas but corresponding to processes with very similar kinetics) is in the case of our data represented by the two finest powder fractions, 0-20 μm and 20-50 μm — this information was, however, obtained only once the deconvolution was performed, i.e., it was not derived by means of advanced interpretation of characteristic kinetic functions.

Based on all this information, the modified Fraser–Suzuki deconvolution was applied. The Peakfit computer program (Systat Software Inc.) was used to perform the deconvolution; the parameters of the resulting FS functions were

obtained through a non-linear optimization method by using the Levenberg–Marquardt algorithm. The minimum of the residual sum of squares, *RSS*, was sought in order to obtain the best fit. The average correlation coefficient for all performed deconvolution fits was 0.9988 ± 0.0009, which corresponds to high quality of the description. In addition to the details given in the previous section, it should be noted that in the case of the fine powder fractions the interval recommended for FS parameter a_3 needed to be extended up to (–0.45; –0.18) to obtain a reasonably good fit, which is an essential requirement for a correct application of this method. Moreover, the fitting procedure was an iteration process, when the input parameters needed to be adjusted so that the optimum fit corresponding to the real physical behavior of the material was obtained. Certain levels of experience and knowledge of kinetics of the studied processes was demanded on the part of the user for the fits to be performed properly. In this regard, information provided within the framework of the advanced $z(\alpha)$ and $y(\alpha)$ interpretation approach was the most beneficial. This will be further addressed, after the results of deconvolution and following kinetic analysis are described.

The kinetic analysis of the deconvoluted peaks is performed in essentially the same way as that of the single (overall) process; i.e., Eq. (1) needs to be solved. Starting with the determination of the crystallization enthalpy ΔH_{cry}, Fig. 5 shows the dependence of the total heat release (summed for both processes) on the heating rate, q^+, and average particle size, d_{aver}. A similar pattern can be found in the case of numerous materials. The decrease in ΔH_{cry} associated with low heating rates most probably results from the energy dissipation due to the heat being released too slowly. Similarly, the decrease associated with fine powder fractions (lower particle size) can possibly also be connected with thermal gradients in samples and resulting heat dissipation, as the initial material was 100 % glassy (derived from the unchanging value of heat capacity change at T_g, verified by XRD). As can be seen in Fig. 5, the difference between crystallization enthalpies is substantial and question remains, whether it can be attributed fully to the dissipation effects. Another explanation might employ different enthalpy changes associated with the two involved crystallization mechanisms (surface and bulk); however, according to the present authors' opinion, such option is of a low probability. Nevertheless, for the kinetic calculations themselves the differences are still insignificant, as the only parameter actually influenced is the pre-exponential factor A, where the error is comparable to those arising during the very measurements.

The interesting variable in this case is the ratio between the two involved crystallization mechanisms. As the overall ΔH_{cry} changes, it is suitable for the data to be plotted in the way shown in Fig. 6, where the percentage of the surface crystallization (expressed as % of the overall peak area) is given in the dependence on the discrete values of the heating rates and average particle sizes (the extreme cases are suggested in the figure). As it is well apparent, in the case of fine powders the surface crystallization clearly dominates and generates major portion of the

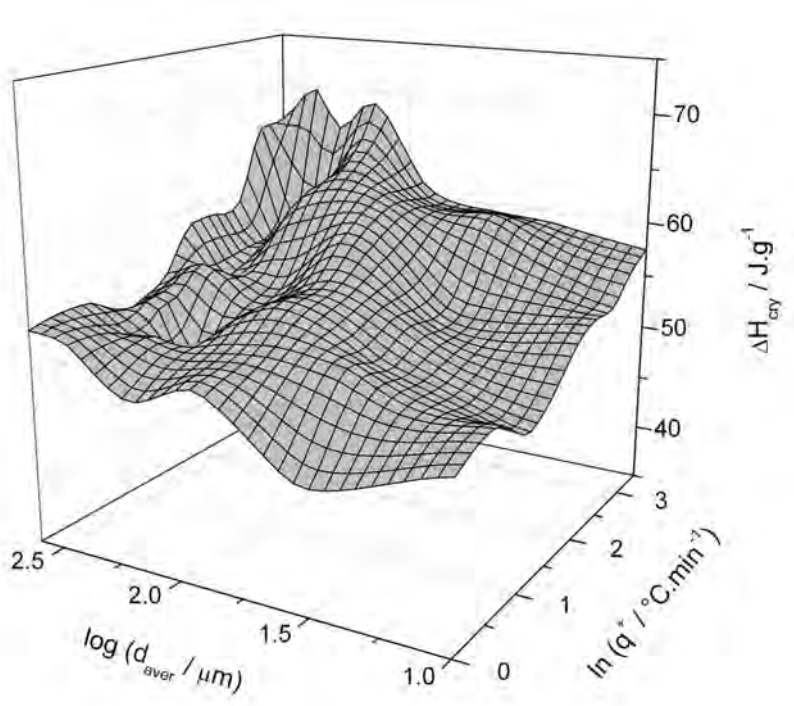

Fig. 5 Overall crystallization enthalpy ΔH_{cry} in dependence on heating rate and averaged particle size

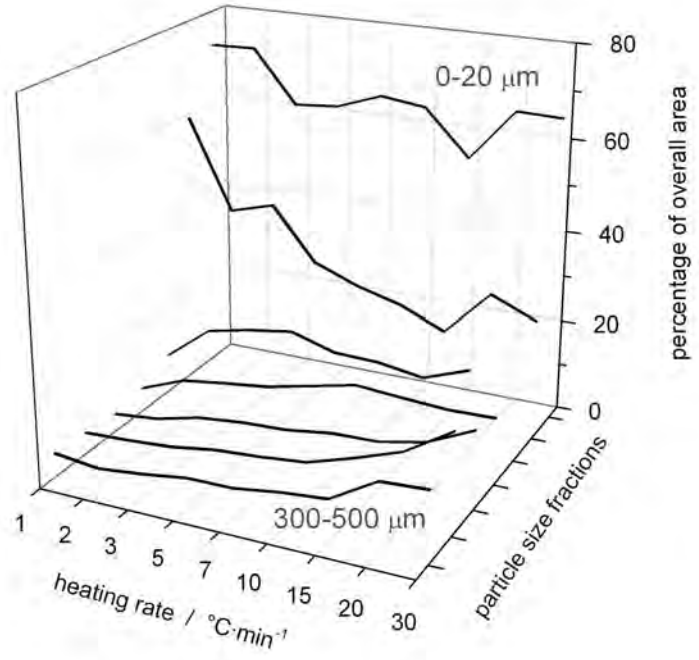

Fig. 6 Percentage of overall crystallization peak area corresponding to surface crystallization in dependence on heating rate for studied particle size fractions. Curves corresponding to two extremes (0-20 μm and 300-500 μm fractions) are suggested

crystallization peak. With the increasing particle size this ratio, naturally, turns in favor of the bulk crystallization — a major part of glass grains is in bulk form.

Nevertheless, even for these very small amounts of the surface crystallization, the trend of increasing ΔH_{cry} with rising q^+, consistent with what was stated in previous text, is apparent. The data for bulk samples are not displayed because of the portion of the surface crystallization being too small to perform a reliable and reasonable deconvolution procedure; in fact each "double-peak fit" resulted in significantly worse correlation coefficient than was that of the bulk crystallization response fitted by a single FS peak. For this reason, the bulk samples were omitted from the following kinetic analysis and only qualitative results are given in the case of this particle size fraction.

The deconvoluted data were further used to construct the respective $z(\alpha)$ and $y(\alpha)$ functions. A comparison with the data prior to deconvolution shows that in the case of the deconvoluted peaks no sign of an additional peak being present is apparent. This fact may be considered as another criterion for a successful and correct deconvolution procedure. If we consider the characteristic kinetic functions themselves, we can see that the $z(\alpha)$ functions are perfectly consistent and with a high accuracy suggest applicability of the JMA model (which was, however, expected as the modified FS deconvolution [31] was used). The high level of correspondence between the experimental and theoretical (0.632) values of $\alpha_{max,z}$ again confirms correctness of the performed deconvolution (provided that the deconvolution fit itself had an acceptable correlation coefficient). If we look closely at the $y(\alpha)$ functions, we can see that the shapes of surface and bulk functions do not differ as significantly as one would assume. This may indicate a larger mutual influencing between the two processes than resulted from the Kissinger plots. This is especially apparent in the case of the bulk process at high heating rates, where evidently the rapidly manifesting surface crystallization controls the overall kinetics. Nevertheless, it could be seen that in average there is still a substantial difference between the two deconvoluted sets of functions, correctly corresponding to the respective crystallization mechanisms — higher average values of $\alpha_{max,z}$ for the bulk crystallization and lower values for the surface mechanism. In general, it can be said that the qualitative description obtained on the basis of the advanced interpretation approach is in good agreement with the results obtained by kinetic analysis of the deconvoluted peaks.

In the last part of the kinetic analysis procedure, the experimental data for each curve were fitted using the JMA model with the corresponding parameter m and activation energy E determined previously; the only variable was the pre-exponential factor A. Examples of such fit are shown in Fig. 7. It can be seen that all fits are very good; in addition, the deconvoluted peaks for each fraction show a standard increase in their magnitude corresponding to the rising heating rate (similar information about consistency of performed deconvolution can be also derived from Fig. 6). Moreover, based on the mutual position of discrete peaks within the framework of each fraction, an approximate piece of information about the type of observed process (coinciding with deconvolution interpretation) can be

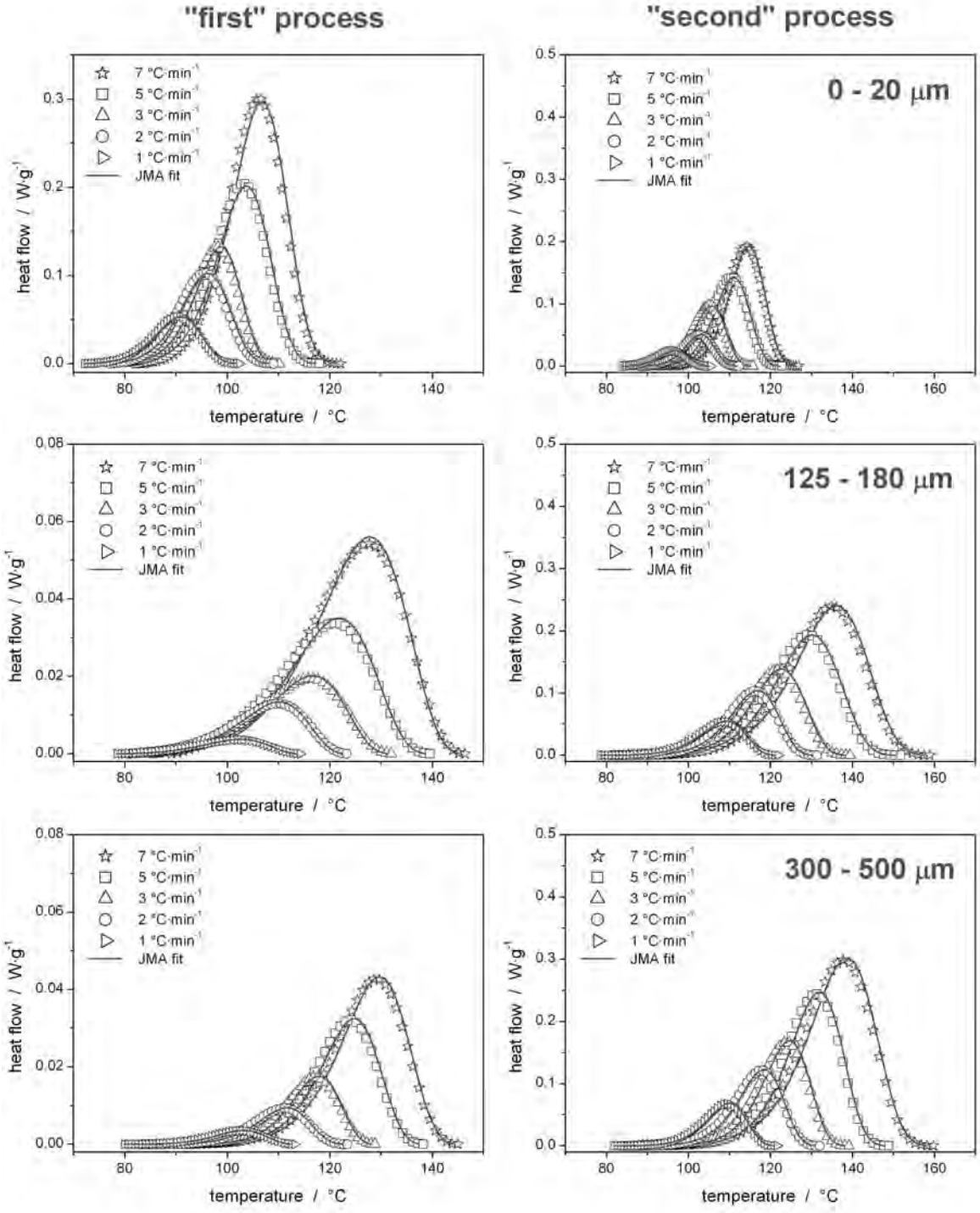

Fig.7 Deconvoluted crystallization peaks corresponding to non-isothermal measurements of chosen particle size fractions of selenium glass performed at low heating rates. Particular rows match individual studied fractions, left column corresponds to surface crystallization mechanism, right column represents data for bulk crystallization process. Solid lines represent fit by JMA model

derived: in the case of the surface crystallization, the peaks for most fractions are very close in their onset and initial edge, which corresponds to the "lower order" kinetics; on the other hand, the peaks for the bulk crystallization mechanism show

a significant shift in their position, which is in agreement with what is expected for a 3-dimensional process. Altogether, it can be concluded that the presented description of crystallization behavior in a-Se seems to be very consistent with no apparent discrepancies; the results of the deconvolution analysis confirm the conclusions obtained from advanced interpretations of the characteristic kinetic functions.

Comparison with Literature Data

In the last section it will be shown that, by using the two above described and discussed approaches, all the discrepancies and queries from the literature may be explained and, moreover, it will be revealed that all the published data are in a good agreement with the above-suggested picture of crystallization behavior in amorphous selenium.

In the first paragraph, the results by Holubová *et al*. [23] will be commented. In this work, bulk samples were measured non-isothermally at the heating rates 5-20 °C min^{-1}; in addition, also isothermal measurements were performed in the 90-120 °C temperature range. For isothermal experiments, the following values were obtained: $\Delta H_{cry} = 65.5 \pm 2.9$ J g^{-1}, $E = 83 \pm 2$ kJ mol^{-1}, $n_{JMA} \sim 3.5$. The value of the kinetic exponent clearly suggests maximal involvement of the bulk crystallization mechanism, which is in a good agreement with our results — a bulk sample measured at the minimum heating rate is the closest experimental setup regarding our results. The slightly higher value of the crystallization enthalpy and slightly lower value of the activation energy may correspond to a larger involvement of the surface crystallization, e.g., due to sample surface being cut, ground, polished, *etc*. (which would not necessarily contradict the previous statement, as in the case of n_{JMA} determination the mutual position of the involved processes can strongly affect the result) or due to the initial fast temperature build-up causing the energy surplus (leading to involvement of surface crystallization mechanism). In the case of non-isothermal measurements, the reported Kissinger activation energy is 64.1 ± 2.5 kJ mol^{-1}, which again corresponds to the evaluation of measurements performed at moderate-to-higher heating rates (see Figs 1 and 2). Regarding the description of the kinetic model, Holubová *et al*. [23] report that the JMA model was suitable for the description of obtained data only in the case of low heating rates; for high heating rates the autocatalytic model [1] had be used. The explanation provided by Holubová *et al*. included an influence of varying temperature-dependent nucleation rate, whereas our results indicate that the deviation from the ideal single-process JMA behavior was caused by involvement of the surface crystallization process manifesting significantly at higher heating rates. This deviation observed in the case of bulk samples again suggests a large amount of surface crystallization centres being present in the material; the origin of these active sites may probably

be associated with the sample preparation procedure.

In the second paragraph, the work by Joraid *et al*. [24] will be reviewed. In this work, fine Se powder was measured non-isothermally by a DSC under a large variety of heating rates 2-99 °C min^{-1}. For this range of heating rates, the reported values of ΔH_{cry} increased from approximately 35 to approx. 57 J g^{-1} — the upper value very well corresponds to our results for high heating rates; on the other hand, the value for low heating rates is significantly lower than that obtained in our study, which might be caused, e.g., by an inaccurate subtraction of baseline in addition to the dissipation effect itself (the data in Ref. [24] seem to vary significantly in their heat capacity and baseline slopes for various heating rates). Furthermore, Joraid *et al*. determined apparent activation energy in the dependence on heating rate — a decrease from approximately 100 to 70 kJ mol^{-1} was observed for the above mentioned heating rate. This again very well corresponds to our results, where the curvature for fine powders is only minimal and for heating rates as high as 99 °C min^{-1} the evaluation may provide results similar to those reported by Joraid *et al*. in Ref. [24]. Lastly, the values and consistency of the maxima of characteristic kinetic functions calculated in [24] also correspond to our results for fine powders. Slightly lower values in the case of very high heating rates are most probably caused by the deformation of the crystallization peaks due to the thermal gradients in samples (confirmed by our own measurements).

Thirdly, in their work [25] Abu-Sehly *et al*. studied isothermal kinetics for a-Se powder samples. A strong dependence of the apparent activation energy, *E,* on the degree of conversion, α, and variation of the Avrami exponent *n* with the annealing temperature (values from 2 to 4 in the 80-100 °C range), together with the fact that the isothermal crystallization proceeded much faster than in the case of the measurements by Holubová *et al*. [23] performed on bulk, suggest that also in the case of isothermal measurements at low temperatures, the surface crystallization proceeds predominantly when the material contains a sufficient number of surface defects acting as crystallization centres.

In the next commented work [26], Afify studied crystallization kinetics for a-Se isothermally and non-isothermally. Unfortunately, the exact form of the sample is not specified. Nevertheless, if we take into account the published values of $E = 79.4$ kJ mol^{-1} (non-isothermally, heating rates 2.5-40 °C min^{-1}) and $n = 1.75$, we can assume that the sample was in the form of coarse powder or bulk pieces with a higher portion of damaged surface. In the case of isothermal measurements, almost similar values as those determined non-isothermally were obtained.

Crystallization in thin selenium films was studied, e.g., in Refs [27] and [28]. Both articles were published by the same research group, in the earlier work [27] Joraid applied rather a broad range of heating rates 2-99 °C min^{-1} in addition to the AFM and SEM studies. The reported activation energy varied to a large extent with both the degree of conversion, α, and temperature, *T*, which corresponds to our findings (implying that also in the case of crystallization in thin films multiple

processes are involved). Despite the authors' statement, the experimental data are in Ref. [27] fitted very poorly for all heating rates, and the single-peak JMA process cannot describe the studied crystallization behaviour. In their next work [28], Joraid *et al*. restate some of their previous conclusions and treat the observed crystallization peaks as a combination of two steps. Unfortunately, the deconvolution was done using Gaussian functions, which distorts and misrepresents the results, even though only the activation energy was calculated for the two particular processes. The reported Kissinger plots show, in the case of both deconvoluted peaks, a similar curvature for high heating rates as that observed in the case of our data. According to the authors, the two peaks can be associated with a formation of two phases — hexagonal and monoclinic (their presence was confirmed by XRD); the curvature in the Kissinger plots is to be caused by a lack of the nucleation activation energy being involved. As the crystallization behaviour in thin films may differ significantly from that in the bulk material, currently it cannot be decided for certain, whether the idea presented by Joraid *et al*. is consistent with the concept presented in our work. Nevertheless, at least partial resemblances are clearly recognizable.

Conclusion

Crystallization kinetics in amorphous selenium was studied under non-isothermal conditions by using differential scanning calorimetry. The main aim of the study was to demonstrate the current level of information obtainable by modern deconvolution procedures in the case of complex crystallization processes. It was shown, that by a combination of the modified Fraser–Suzuki deconvolution and advanced interpretation of characteristic kinetic functions $z(\alpha)$ and $y(\alpha)$, the complete picture about crystallization kinetics in a given material can be gained. This was proved in the last part of the Results and Discussion section, where random results from literature were taken and explained on the basis of the overall concept generated within the framework of this article. In addition, from the non-isothermal measurements, a very good conceptual description was obtained also for the results of isothermal measurements or experiments performed on thin films.

The key/base principles are the following: the kinetic analysis performed with respect to changing particle size; precise and reproducible DSC measurements; derivation of maximum amount of reliable information about the process; accurate deconvolution with a high correlation coefficient that is performed on the basis of prior knowledge of the process.

It is the main advantage of the approach introduced in this article that it is in fact general, suggestive and relatively easily applicable to any possible amorphous material, the crystallization of which can be observed by the DSC technique. As the crystallization process is of a crucial importance in numerous

modern applications (crystallization has to be either avoided in order to obtain perfect and stable glass with finest optical or electrical properties or, on the contrary, the crystallization process in a glassy matrix is in the fact the fundamental basis of the technology), an accurate and complete description taking into account complexity of this process may be of high value. In this regard, the introduced approach can play an important role in development and testing of various new and promising hi-tech materials, and as such represents a true interconnection between the thermal analysis and material science.

Acknowledgement

This work was supported by the Czech Science Foundation under project No. P106/11/1152.

References

[1] Šesták J.: *Thermophysical Properties of Solids, Their Measurements and Theoretical Analysis*, Elsevier, Amsterdam, 1984.
[2] Kissinger H.E.: Anal. Chem. **29**, 1702 (1957).
[3] Friedman H.L.: *Kinetics of Thermal Degradation of Char-Forming Plastics from Thermogravimetry*, Wiley Company, New York, 1964.
[4] Málek J.: Thermochim. Acta **355**, 239 (2000).
[5] Málek J.: Thermochim. Acta **200**, 257 (1992).
[6] Avrami M.: J. Chem. Phys. **7**, 1103 (1939).
[7] Avrami M.: J. Chem. Phys. **7**, 212 (1940).
[8] Avrami M.. J. Chem. Phys. **7**, 177 (1941).
[9] Johnson W.A., Mehl K.F.: Trans. Am. Inst. Min. (Metall.) Eng. **135**, 416 (1939).
[10] Málek J.: Thermochim. Acta **138**, 337 (1989).
[11] Šesták J: *Science of Heat and Thermophysical Studies: A Generalized Approach to Thermal Analysis*, Elsevier, Amsterdam (2005).
[12] Svoboda R., Málek J.: J. Therm. Anal. Calorim. DOI:10.1007/s10973-012-2347-x (2012).
[13] Gotor F.J., Criado J.M., Malek J., Koga N.: J. Phys. Chem. A **104**, 10777 (2000).
[14] Sempere J., Nomen R., Serra R., Soravilla J.: Thermochim. Acta **388**, 407 (2002).
[15] Sempere J., Nomen R., Serra R.: J. Therm. Anal. Cal. **56**, 843 (1999).
[16] Sanchez-Jimenez P.E., Perez-Maqueda L.A., Perejon A., Criado J.M.: Polym. Degrad. Stab. **94**, 2079 (2009).

[17] Perez-Maqueda L.A., Criado J.M., Malek J.: J. Non-Cryst. Sol. **320**, 84 (2003).
[18] Lesnikovich A.I., Levchik S.V.: J. Therm. Anal. **27**, 89 (1983).
[19] Lesnikovich A.I., Levchik S.V.: J. Therm. Anal. **30**, 677 (1985).
[20] Perejón A., Sánchéz-Jiménez P.E., Criado J.M., Pérez-Maqueda L.A.: J. Phys. Chem. B **115**, 1780 (2011).
[21] Fraser R.D.B., Suzuki E.: Anal. Chem. **38**, 1770 (1966).
[22] Fraser R.D.B., Suzuki E.: Anal. Chem. **61**, 37 (1969).
[23] Holubová J., Černošek Z., Černošková E., Černá A.: Mater. Lett. **60**, 2429 (2006).
[24] Joraid A.A., Alamri S.N., Abu-Sehly A.A.: J. Non-Cryst. Sol. **354**, 3380 (2008).
[25] Abu-Sehly A.A., Alamri S.N., Joraid A.A.: J. Alloys Compd. **476**, 348 (2009).
[26] Afify N.: J. Phys. Chem. Sol. **69**, 1691 (2008).
[27] Joraid A.A.: Physica B **390**, 263 (2007).
[28] Joraid A.A., Abu-Sehly A.A., Alamri S.N.: Thin Sol. Films **517**, 6137 (2009).
[29] Svoboda R., Málek J.: Thermochim. Acta **526**, 237 (2011).
[30] Svoboda R., Málek J.: J. Non-Cryst. Sol. **358**, 276 (2012).
[31] Svoboda R., Málek J.: J. Therm. Anal. Calorim. DOI 10.1007/s10973-012-2445-9 (2012).